

Optimal Design of Double-Walled Corrugated Board Packaging

Damian Mrówczyński ¹, Anna Knitter-Piątkowska ² and Tomasz Garbowski ^{3,*}

¹ Doctoral School, Department of Biosystems Engineering, Poznan University of Life Sciences, Wojska Polskiego 28, 60-637 Poznań, Poland; damian.mrowczynski@up.poznan.pl

² Institute of Structural Analysis, Poznan University of Technology, Piotrowo 5, 60-965 Poznań, Poland; anna.knitter-piatkowska@put.poznan.pl

³ Department of Biosystems Engineering, Poznan University of Life Sciences, Wojska Polskiego 50, 60-627 Poznań, Poland

* Correspondence: tomasz.garbowski@up.poznan.pl

Abstract: Designing corrugated board packaging is a real challenge, especially when the packaging material comes from multiple recycling. Recycling itself is a pro-ecological and absolutely necessary process, but the mechanical properties of materials that are processed many times deteriorate with the number of cycles. Manufacturers are trying to use unprecedented design methods to preserve the load-bearing capacity of packaging, even when the material itself is of deteriorating quality. An additional obstacle in the process of designing the structure of paper packaging is the progressive systematic reduction of the grammage (the so-called lightweight process) of corrugated cardboard. Therefore, this research presents a critical look at the process of optimal selection of corrugated cardboard for packaging structures, depending on the paper used. The study utilizes analytical, simplified formulas to estimate the strength of cardboard itself as well as the strength of packaging, which are then analyzed to determine their sensitivity to changes in cardboard components, such as the types of paper of individual layers. In the performed sensitivity analysis, numerical homogenization was used, and the influence of initial imperfections on the packaging mechanics was determined. The paper presents a simple algorithm for the optimal selection of the composition of corrugated cardboard depending on the material used and the geometry of the packaging, which allows for a more conscious production of corrugated cardboard from materials derived, e.g., from multiple recycling.

Keywords: non-local sensitivity analysis; numerical homogenization; optimal packaging; box compressive strength; critical load; orthotropic plate; edge crush resistance; bending stiffness; corrugated cardboard



Citation: Mrówczyński, D.; Knitter-Piątkowska, A.; Garbowski, T. Optimal Design of Double-Walled Corrugated Board Packaging. *Materials* **2022**, *15*, 2149. <https://doi.org/10.3390/ma15062149>

Academic Editor: Zhengming Huang

Received: 28 February 2022

Accepted: 14 March 2022

Published: 15 March 2022

Publisher's Note: MDPI stays neutral with regard to jurisdictional claims in published maps and institutional affiliations.



Copyright: © 2022 by the authors. Licensee MDPI, Basel, Switzerland. This article is an open access article distributed under the terms and conditions of the Creative Commons Attribution (CC BY) license (<https://creativecommons.org/licenses/by/4.0/>).

1. Introduction

According to the *Paper and Paperboard Packaging Market* report [1], the sector of global paper industry in 2021 was estimated to value USD 199.8 billion and is forecasted to attain USD 254.5 billion by 2026, at a Compound Annual Growth Rate (CAGR) of 5.0% during the term of reference. Such a tremendous growth is driven, among others, by a huge demand of paper packaging material in the pharmaceutical, cosmetics, food, and beverage industry. Amid the COVID-19 crisis, consumer habits have changed considerably, leading to a strong speedup of e-commerce shipments and other home delivery services, which have impacted the packaging industry by increasing the need for paper and cardboard containers.

The current environmental pollution is also a good trigger for the development of the corrugated board market in view of the fact that cellulose packaging is widely believed to be highly ecological; therefore, a shift has occurred from the use of plastic to that of paper and paperboard. Corrugated cardboard packaging companies focus also on shelf-ready packaging (SRP) or retail-ready packaging (RRP), which significantly improves unpacking and displaying products in stores. Thanks to this, brands have an excellent opportunity to

shape the store space more independently and to distinguish their products with original printed packaging.

The high requirements of such a demanding market with strong competition promote manufacturers' interest in finding innovative solutions for paper/cardboard components and the use of kraft or recycled paper and new packaging designs, e.g., by facilitating product returns or lighter fluting and allowing for a reduction in the dimensions, weight, as well as cost of the packages, provided that the boxes are of adequate load-bearing capacity. Corrugated cardboard is a layered structure whose strength is determined by the individual ply selection and combination, especially given the fact that the mechanical strength of paperboard depends on two characteristic, i.e., the in-plane directions of orthotropy—perpendicular to the main axis of the fluting and parallel to the paperboard fiber alignment machine direction (MD), as well as parallel to the fluting cross direction (CD). This paper presents a critical look at the process of optimal selection of five-layer corrugated cardboard for packaging structures, depending on the paper used, as a continuation of the discussion presented for three-ply cardboard by Mrówczyński et al. [2].

Taking into account all the above-mentioned conditions, the natural consequence of the development of the cardboard packaging market is a rapid and intensive progress in scientific research in this field. Scientists all over the world, through the years, have been proposing a great deal of methods for the estimation of cardboard load-bearing capacity. In a broad sense, one can distinguish analytical, numerical, and experimental approaches.

Analytical methods were proposed as early as in the 1950s [3–5] and identify paper, board, and box parameters [6] using formulae. To the first group of parameters belong the ring crush test (RCT), the Concora liner test (CLT), the liner type, the weights of liner and fluting, the corrugation ratio, and a constant related to fluting. The second one includes thickness, flexural stiffnesses in MD and CD, the results of the edge crush test (ECT), and moisture, whereas the third one comprises the dimensions and perimeter of the box, the applied load ratio, the stacking time, and the buckling and printed ratios. Fast and simple solutions for practical applications in the packaging industry can be found by employing the McKee analytical formula [5], which is commonly used but is only applicable to simple standard boxes. Therefore, this approach is still being developed, and numerous studies have focused on, e.g., the modification of constants and exponents, the expansion of the range of cutting methods and equipment [7], the introduction of the dimensions of the box [8], or the incorporation of the Poisson's ratio [9]. A further improvement of the above approach to solve more complex problems was presented in Avilés et al. [10]. The buckling phenomena of the orthotropic cardboards were examined in Garbowski and Knitter-Piątkowska [11], and, recently, the analytical determination of the bending stiffness (BS) of a five-layer corrugated cardboard with imperfections was discussed in [12].

A recognized and valued numerical technique is the finite element method (FEM), also in terms of cardboard strength assessment. Some studies discussed the mechanical properties of cardboard during the FEM simulation of creasing [13–18], whereas others performed numerical strength estimations of corrugated board packages [19–22]. The cohesive zone method has been applied for the stress analysis in adhesively bonded joints of the corrugated sandwich structure [23] and for the prediction of the mechanical degradation of the corrugated sandwich beam [24], with verification of the results by FEM. FEM has also been employed to examine the torsional and transversal stiffness of orthotropic paper materials [25–27] and the bending stiffness [28,29] and buckling or post-buckling phenomena [30] of cardboard.

Finite element analysis of hot melt adhesive joints in carton board was performed by Hallbäck et al. [31]. Because of the anisotropy of paper materials and the layered structure of cardboards, carrying out numerical simulations is a challenging task, since it is necessary to know the material parameters of each layer. A remedy to this situation is a procedure called homogenization. This method consists in determining the equivalent stiffnesses and effective thicknesses of a model, which allows to reduce the layered structure to one single layer.

The equations of the classical theory of strength of materials or the classical theory of laminates lie at the root of analytical homogenization [32], whilst numerical homogenization is based on the FEM. In this approach, first, a numerical model of a representative volume element (RVE) is created [33]. The use of asymptotic homogenization was presented [34,35]. In case of a corrugated board, the homogenization may be conducted in two ways, i.e., homogenization to one layer or homogenization of fluting to the inner layer of the laminate. This procedure has been widely utilized in recent years [36–45] because of a significant saving in computation time while preserving the precision of the results.

Experimental measurements performed to determine the strength of corrugated boards are commonly performed in the paper industry. Compressive, tensile, or bursting strength tests are the main physical examinations carried out. The most common are the box compression test (BCT), the bending stiffness (BS), and the edge crush test (ECT) [12,46–48]. The crushing of single- and double-walled corrugated boards was discussed in Gajewski et al. [49] and Garbowski et al. [50]. Moreover, the bending test (BNT), the shear stiffness test (SST), and the torsional stiffness test (TST) are also relevant. Bursting and humidity testing are performed as well.

The method called video extensometry allows gathering data from the exterior surface of the specimen. During the testing, the relative distances between pairs of points tracked on images registered at different force values are measured [51,52]. This procedure is comparable to digital image correlation (DIC), which is a full-field non-contact optical measurement technique, yet it is simpler. A significant advantage of this method is the very high accuracy of data capture, which has made it valuable in the field of experimental mechanics [27,53–58].

Cardboard is ideal for shaping packaging material; however, one has to bear in mind that there are many factors that reduce its load-bearing capacity [59]. These include the presence of ventilation holes and perforations or indentations [60–64], shifted creases on flaps [65], time and conditions of storage [66,67], and the stacking load [42,68,69]. The risk of failure to meet the guaranteed load-bearing capacity cannot be disregarded. When evaluating the strength of cardboard packaging, one has to take into account the influence of box geometry and the composition as well as the arrangement of the corrugated board layers on the change of the buckling force, edge crushing (ECT), and compressive box strength resistance (BCT). Important is the fact that the behavior of cardboard strictly depends on its dimensions, i.e., for tall packaging, the buckling strength is crucial, while for low and stocky boxes, a high edge crush strength is essential.

The optimum choice of the composition of the corrugated board layers is of utmost importance for the load capacity of the packaging. The procedure described in this paper makes it possible to identify the components that affect the strength of packages of diverse dimensions and to estimate their effect. The study utilizes analytical, simplified formulas to estimate not only the strength of cardboard itself, but also the strength of packaging. These parameters are then analyzed to determine their sensitivity to changes in the cardboard components, namely, the types of paper of individual layers. In the performed sensitivity analysis, numerical homogenization and the study of the influence of initial imperfections on the packaging mechanics were carried out. The use of non-local sensitivity analysis allowed for a critical look at the process of optimal selection of corrugated cardboard for the packaging structure, depending on the paper used. A novelty that distinguishes the presented research from others is the proposed, complete algorithm for the optimal selection of the components of a five-layer corrugated cardboard depending on the material used and the geometry of the packaging.

2. Materials and Methods

2.1. Material Parameters and Corrugated Cardboard Geometry

Corrugated cardboard is highly orthotropic, mainly due to the fact that it is a fibrous material. Its mechanical properties depend on the orientation of the fibers in the corrugated cardboard layers. Most fibers run along the paper web, which is called the machine direction

(MD). The second main direction is the direction perpendicular to the MD, called the cross direction (CD), see Figure 1. Corrugated cardboard, because of its fiber orientation, is stiffer along the wave direction. Weaker mechanical properties in the CD are compensated by the take-up factor of the corrugated layers.

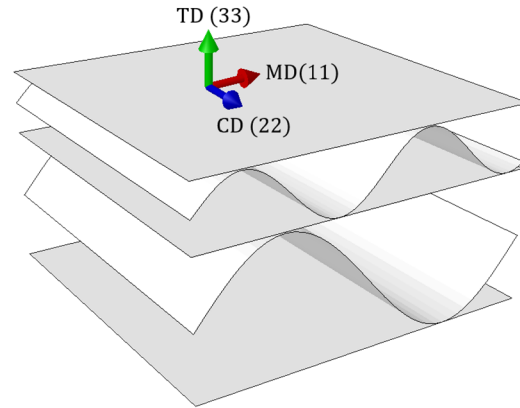


Figure 1. Material orientation. Machine direction (MD), cross direction (CD), and thickness direction (TD). The notation 1, 2, 3 refers to the principal orthotropic directions.

The most important mechanical properties of corrugated board are the moduli of elasticity in the machine and cross directions, E_1 and E_2 , respectively, and the compressive strength in the cross direction SCT_{CD} . They can be calculated based on the grammage of the paper while using the MONDI specifications [70]. The method of determining the mechanical properties is shown below (see Table 1). Both moduli of elasticity can be calculated from the formulas:

$$E_1 = TS_{MD} \frac{grm}{thk}, \quad E_2 = TS_{CD} \frac{grm}{thk}, \quad (1)$$

where TS_{MD} and TS_{CD} are the tensile stiffness indexes in MD and CD (Nmm/g), thk is the thickness of the paper (mm), and grm is the paper grammage (g/m^2). It is assumed that the paper thickness equals to 160 μm and corresponds to a grammage of 100 g/m^2 .

Table 1. MONDI technical data for kraftliner paper.

Property	Unit of Measure	Grammage (g/m^2)								
		100	110	125	135	150	160	170	186	200
SCT_{CD}	N/mm	2.0	2.3	2.5	2.7	3.0	3.2	3.4	3.7	4.0
Tensile stiffness index $_{MD}$	Nmm/g			11				12		
Tensile stiffness index $_{CD}$	Nmm/g					5				

The remaining parameters necessary to describe the orthotropic material can be directly determined from the moduli of elasticity E_1 and E_2 . The Poisson’s ratio ν_{12} and the in-plane shear stiffness G_{12} can be calculated from the empirical formulas [71]:

$$\nu_{12} = 0.293 \sqrt{\frac{E_2}{E_1}}, \quad G_{12} = 0.387 \sqrt{E_1 E_2}. \quad (2)$$

The transverse shear stiffnesses are approximated by the formulas [72]:

$$G_{13} = \frac{E_1}{55}, \quad G_{23} = \frac{E_2}{35}. \quad (3)$$

The geometric parameters of the waves, such as height, period, and take-up factor, are selected based on the wave type, as shown in Table 2.

Table 2. Geometric parameters of waves.

Wave (Flute)	Wave Length (mm)	Height (mm)	Take-Up Factor (-)
B	6.5	2.46	1.32
C	8.0	3.61	1.43
E	3.5	1.15	1.27

2.2. Homogenization Technique

The full 3D model of cardboard, very burdensome in numerical calculations, can be simplified to a single layer with equivalent mechanical properties by means of numerical homogenization. In this paper, a method based on elastic energy equivalence proposed by Biancollini [33] and extended by Garbowski and Gajewski [45] is presented. This method uses a representative volume element (RVE), i.e., a small and periodic fragment of the entire corrugated cardboard structure, which is then transformed into a simplified shell model. The most important information on the applied homogenization method is presented below. The entire theoretical derivation can be found in [45]. The basic equation of the linear finite element method is as follows:

$$\mathbf{K}_e \mathbf{u}_e = \mathbf{F}_e, \quad (4)$$

where \mathbf{K}_e is a global stiffness matrix condensed to the external nodes of the RVE, \mathbf{u}_e is a displacement vector, and \mathbf{F}_e is a vector of nodal forces. The subscript e indicates values in the RVE external nodes. In Figure 2, the finite element mesh and external nodes of the RVE are presented.

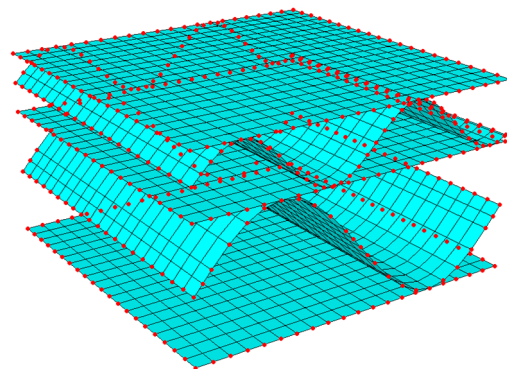


Figure 2. Finite elements and nodes (external, in red color) of the RVE of a double-walled corrugated board.

In order to compute the condensed stiffness matrix, static condensation needs to be used, which removes certain unknown degrees of freedom (DOF) and only leaves the important degrees of freedom, known as primary unknowns. In the analyzed case, external nodes were left, and internal nodes were removed. The global stiffness matrix was condensed to the external nodes while applying the following formula:

$$\mathbf{K}_e = \mathbf{K}_{ee} - \mathbf{K}_{ei} \mathbf{K}_{ii}^{-1} \mathbf{K}_{ie}, \quad (5)$$

where the subarrays represent the stiffness matrices of the internal (subscript i) and external (subscript e) nodes:

$$\begin{bmatrix} \mathbf{K}_{ee} & \mathbf{K}_{ei} \\ \mathbf{K}_{ie} & \mathbf{K}_{ii} \end{bmatrix} \begin{bmatrix} \mathbf{u}_e \\ \mathbf{u}_i \end{bmatrix} = \begin{bmatrix} \mathbf{F}_e \\ \mathbf{0} \end{bmatrix}. \quad (6)$$

After condensation of the model to the external nodes, the total strain energy became equal to the work of external forces on the corresponding displacements:

$$E = \frac{1}{2} \mathbf{u}_e^T \mathbf{F}_e. \quad (7)$$

The presented method utilizes the principle that total energy balance between the full 3D model and the simplified shell model must be ensured. For this reason, it was necessary to appropriately determine the displacements and define the membrane and bending behavior [45]. There is a relationship between the generalized displacements and the generalized strains in the external nodes of the RVE:

$$\mathbf{u}_i = \mathbf{H}_i \boldsymbol{\varepsilon}_i, \quad (8)$$

where the \mathbf{H}_i matrix is defined by the coordinates of each node ($x_i = x, y_i = y, z_i = z$):

$$\begin{bmatrix} u_x \\ u_y \\ u_z \\ \theta_x \\ \theta_y \end{bmatrix}_i = \begin{bmatrix} x & 0 & y/2 & xz & 0 & yz/2 & z/2 & 0 \\ 0 & y & x/2 & 0 & yz & xz/2 & 0 & z/2 \\ 0 & 0 & 0 & -x^2/2 & -y^2/2 & -xy/2 & x/2 & y/2 \\ 0 & 0 & 0 & 0 & -y & -x/2 & 0 & 0 \\ 0 & 0 & 0 & x & 0 & y/2 & 0 & 0 \end{bmatrix}_i \begin{bmatrix} \varepsilon_x \\ \varepsilon_y \\ \gamma_{xy} \\ \kappa_x \\ \kappa_y \\ \kappa_{xy} \\ \gamma_{xz} \\ \gamma_{yz} \end{bmatrix}_i. \quad (9)$$

The transformation matrix, \mathbf{H}_i , allows relating the generalized displacements to the generalized strains in external nodes of the RVE model. Details on the derivation of the transformation matrix can be found in [33] for the Kirchhoff–Love theory and in [45] for Reissner–Minding plates. Considering the elastic strain energy equation:

$$E = \frac{1}{2} \mathbf{u}_e^T \mathbf{K} \mathbf{u}_e = \frac{1}{2} \boldsymbol{\varepsilon}_e^T \mathbf{H}_e^T \mathbf{K} \mathbf{H}_e \boldsymbol{\varepsilon}_e \quad (10)$$

and analyzing the basic load states, such as bending, tension, and transverse shear, the elastic internal energy can be determined as:

$$E = \frac{1}{2} \boldsymbol{\varepsilon}_e^T \mathbf{H}_k \boldsymbol{\varepsilon}_e \{area\}. \quad (11)$$

The stiffness matrix for the homogenized RVE of the corrugated cardboard can be computed from:

$$\mathbf{H}_k = \frac{\mathbf{H}_e^T \mathbf{K} \mathbf{H}_e}{area}. \quad (12)$$

The \mathbf{H}_k matrix includes the stiffness matrices \mathbf{A} , \mathbf{B} , \mathbf{D} , and \mathbf{R} as shown below:

$$\mathbf{H}_k = \begin{bmatrix} \mathbf{A}_{3 \times 3} & \mathbf{B}_{3 \times 3} & 0 \\ \mathbf{B}_{3 \times 3} & \mathbf{D}_{3 \times 3} & 0 \\ 0 & 0 & \mathbf{R}_{2 \times 2} \end{bmatrix}, \quad (13)$$

where the subarray \mathbf{A} represents tensile and shear stiffnesses, the subarray \mathbf{B} represents the matrix linking tensile and bending stiffnesses, the subarray \mathbf{D} contains bending and torsional stiffnesses, and the subarray \mathbf{R} represents transverse shear stiffnesses.

The matrix \mathbf{B} for symmetrical cross sections is the zero matrix. In the case of asymmetrical double-walled corrugated cardboards, which is the subject of the work, non-zero components appear in matrix \mathbf{B} , which subsequently affects the values of matrix \mathbf{D} . This problem can be solved by selecting a neutral axis that minimizes matrix \mathbf{B} . The uncoupled matrix \mathbf{D} can also be determined from the following formula:

$$\mathbf{D} = \mathbf{D}' - \mathbf{B} \mathbf{A}^{-1} \mathbf{B}, \quad (14)$$

where \mathbf{D}' represents bending and torsional stiffnesses for non-zero matrix \mathbf{B} .

2.3. Edge Crush Test (ECT)

Analytically, the ECT value, used to calculate the BCT value, can be determined as the sum of the strength of all layers, taking into account the take-up factor of the waves:

$$ECT = \sum_{i=1}^n p_{max}^i \alpha_i, \tag{15}$$

where p_{max}^i is the maximum load of the i -th layer, and α_i is the take-up factor (see Table 2). The maximum load of the layer can be the critical load P_{cr}^i or the compressive strength SCT_{CD}^i , whichever is achieved first (see Figure 3). The maximum load is:

$$p_{max}^i = \min(SCT_{CD}^i, P_{cr}^i). \tag{16}$$

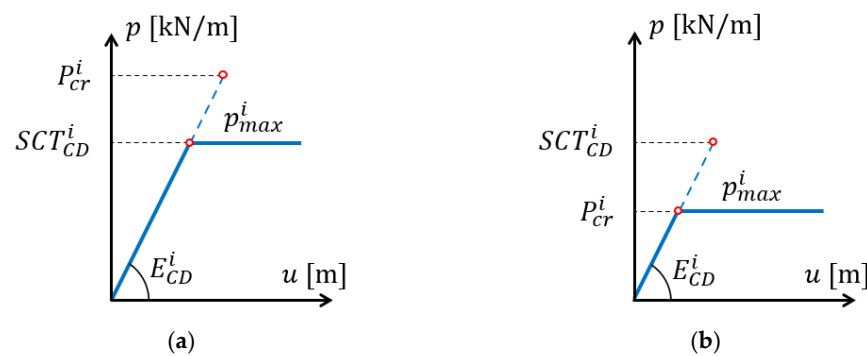


Figure 3. Maximum load of the i -th layer: (a) case where the compressive strength occurs first; (b) case where the critical load occurs first.

The critical load can be determined in many ways, taking into account various factors. An overview of possible cases was presented by Garbowski et al. [11]. For the ECT calculations, the critical load value for rectangular orthotropic panels can be determined from a simplified formula:

$$P_{cr}^L = \frac{1}{\alpha^2} \left[D_{11}\alpha^4 + 2(D_{12} + 2D_{33})\alpha^2\beta^2 + D_{22}\beta^4 \right], \tag{17}$$

where:

$$\alpha = \frac{m\pi}{H}, \quad \beta = \frac{\pi}{L}, \tag{18}$$

$$D_{11} = \frac{1}{w} E_1 I, \quad D_{22} = \frac{1}{w} E_2 I, \tag{19}$$

$$D_{12} = \frac{\nu_{21}}{w} E_1 I = \frac{\nu_{12}}{w} E_2 I, \quad D_{33} = G_{12} I, \tag{20}$$

$$I = \frac{t^3}{12}, \quad w = 1 - \nu_{12}\nu_{21}, \tag{21}$$

where m is the number of half-waves for which P_{cr}^L reaches the minimum, E_1 and E_2 are the moduli of elasticity in MD and CD, respectively, ν_{12} and ν_{21} are the Poisson’s coefficients in the plane, G_{12} is the in-plane shear modulus, and t is the thickness of the panel.

2.4. Box Compression Test (BCT)

The compressive strength can be calculated using the ECT value and the critical loads of the packaging walls. For a rectangular package, the BCT value can be determined from the following formula:

$$BCT = ECT^{0.75} \left[\gamma_L \left(P_{cr}^L \right)^{0.25} L + \gamma_B \left(P_{cr}^B \right)^{0.25} B \right], \tag{22}$$

where γ_L and γ_B are the reduction coefficients, and P_{cr}^L and P_{cr}^B are the critical loads of the packaging walls. The reduction coefficients can be computed from the following formulas:

$$\begin{aligned} \gamma_L &= \sqrt{\frac{L}{B}}, & \gamma_B &= 1, & \text{if } L \leq B, \\ \gamma_L &= 1, & \gamma_B &= \sqrt{\frac{B}{L}}, & \text{if } L > B. \end{aligned} \quad (23)$$

In the case of a relatively thick corrugated cardboard (high waves or double-walled cardboards) and low transverse shear modulus (due to unintentional crushing or the lamination process), it is crucial to take into account the transverse shear stiffness in the calculation of the critical loads of the packaging walls. The transverse shear stiffness is included in the equation:

$$P_{cr}^L = \frac{1}{\alpha^2} \frac{M}{N}, \quad (24)$$

where:

$$M = D_{11}\alpha^4 + 2(D_{12} + 2D_{33})\alpha^2\beta^2 + D_{22}\beta^4 + \left(\frac{\alpha^2}{R_{44}} + \frac{\beta^2}{R_{55}}\right)c_1, \quad (25)$$

$$N = 1 + \frac{c_1}{R_{44}R_{55}} + \frac{c_2}{R_{55}} + \frac{c_3}{R_{44}}, \quad (26)$$

$$c_1 = c_2c_3 - c_4^2 > 0, \quad (27)$$

$$c_2 = D_{11}\alpha^2 + D_{33}\beta^2, \quad (28)$$

$$c_3 = D_{33}\alpha^2 + D_{22}\beta^2, \quad (29)$$

$$c_4 = (D_{12} + D_{33})\alpha\beta. \quad (30)$$

2.5. Bending Stiffness with Imperfections

In the above buckling formulas (Equations (25)–(30)), the bending stiffnesses D_{11} and D_{22} are present, which in the case of a corrugated board with an unsymmetrical cross section, may slightly differ depending on the bending direction (sign of the bending moment). This case was analyzed and presented by Garbowski and Knitter-Piątkowska [12] for a five-ply corrugated board bent in MD (i.e., D_{11} stiffness). The main reason for the disparities is the different number of compressed flat layers, which, in the presence of even very small imperfections, cause noticeable discrepancies in bending stiffness. The bending stiffness in MD can be computed from:

$$D_{11} = \sum_{i=1}^N \frac{E_{1,i}t_i\delta_i}{1 + 6f_i^2t_i^{-2}} \frac{z_i}{\phi}, \quad (31)$$

where $E_{1,i}$ is the Young's modulus in MD of i -th liner, t_i is thickness of i -th liner, δ_i is the axial deformation of i -th liner, z_i is the distance from the i -th liner to the neutral axis of the entire cross section, f_i is an initial imperfection of the i -th liner, ϕ is the rotation of the cross section. It is worth noting that in the case of bending of asymmetrical sections, the value of f_i is different from zero only for the liners that are in compression. In a similar way, one can derive the stiffness in CD, i.e., D_{22} :

$$D_{22} = \sum_{i=1}^N \frac{E_{2,i}t_i\delta_i}{1 + 3f_i^2t_i^{-2}} \frac{z_i}{\phi}. \quad (32)$$

Using the above formulations, two different values of bending stiffness, in both the MD and the CD directions, are obtained. Therefore, both cases should be taken into account when calculating the critical load in Equation (24), depending on the direction of the initial imperfections of the entire corrugated board.

2.6. Non-Local Sensitivity Analysis

The non-local sensitivity of corrugated cardboard was tested for edgewise crush resistance (ECT), box compressive strength (BCT), and critical loads of packaging walls (P_{cr}). The model parameters were the grammage of the corrugated cardboard layers or the bending stiffnesses D_{11} i D_{22} , which were placed in the vector \mathbf{x} . The sensitivity at a specific point in the parameter space can be calculated by determining a numerical gradient while using, e.g., the central difference, according to the formula:

$$s = \frac{h(\mathbf{x} + \mathbf{e}_i \Delta x_i) - h(\mathbf{x} - \mathbf{e}_i \Delta x_i)}{2\Delta x_i} \frac{x_i}{h(\mathbf{x})} \quad (33)$$

where $h(\mathbf{x})$ is the quantity for which the sensitivity is determined (ECT, BCT or P_{cr}), Δx_i is a small perturbation of the i -th parameter, $h(\mathbf{x} - \mathbf{e}_i \Delta x_i)$ is the change of the determined quantity, and \mathbf{e}_i is the unit vector of the i -th parameter in the vector \mathbf{x} .

In the above description, the term 'non-local' means that information about the gradients of the studied quantities is collected in the full range of the analyzed parameter at many points in the parameter space, not only locally at one point in this space. Figure 4 shows an algorithm for the determination of the non-local sensitivity. In the flowchart, i is the number of iterations, and n is the total number of the perturbing parameters.

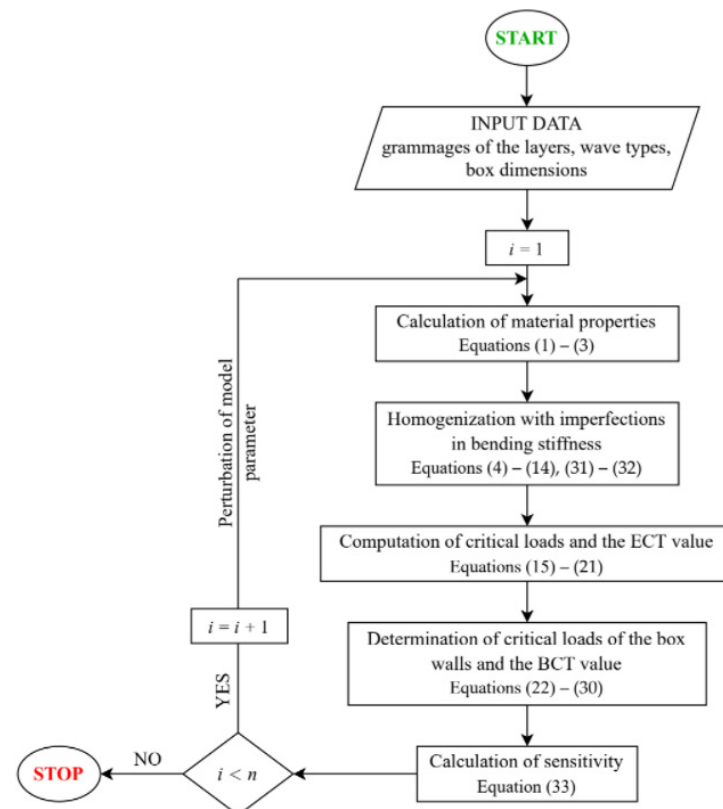


Figure 4. Flowchart of the algorithm for the determination of the non-local sensitivities of a five-ply corrugated board.

3. Results

The most effective tool for determining the optimal layer configuration of a multi-ply corrugated board for packaging is the non-local sensitivity analysis. With its help, it is possible to check which layers (e.g., what basis weight, what type of paper) work best and in which packaging structures. All sensitivity values presented below were computed from Equation (33), where the variable h indicated ECT, P_{cr} , or BCT values. First, we analyzed the sensitivity of ECT, the value of which was calculated from Equation (15). The ECT value is influenced by the stiffnesses in the machine (MD) and cross (CD) directions and

by the compressive strength in the CD (through the critical load). It follows that the ECT value depends on the grammage of the cardboard layers, see Equation (1).

Four double-walled corrugated cardboards (BC, EB, EC, EE) for different combinations of layer grammage were analyzed. The combinations were based on liners grammage from 100 every 20 to 200 g/m² and fluting grammage from 80 every 20 to 160 g/m², which gave in total 5400 combinations for each cardboard.

In Figure 5, the sensitivity of ECT to the change in grammage of the cardboard layers is presented. The median values are marked by red horizontal lines, and the bottom and top blue edges of the box indicate the 25th and 75th percentiles, respectively. The whiskers extend to the most extreme data points not considered outliers, and the outliers are plotted individually using the '+' marker symbol.

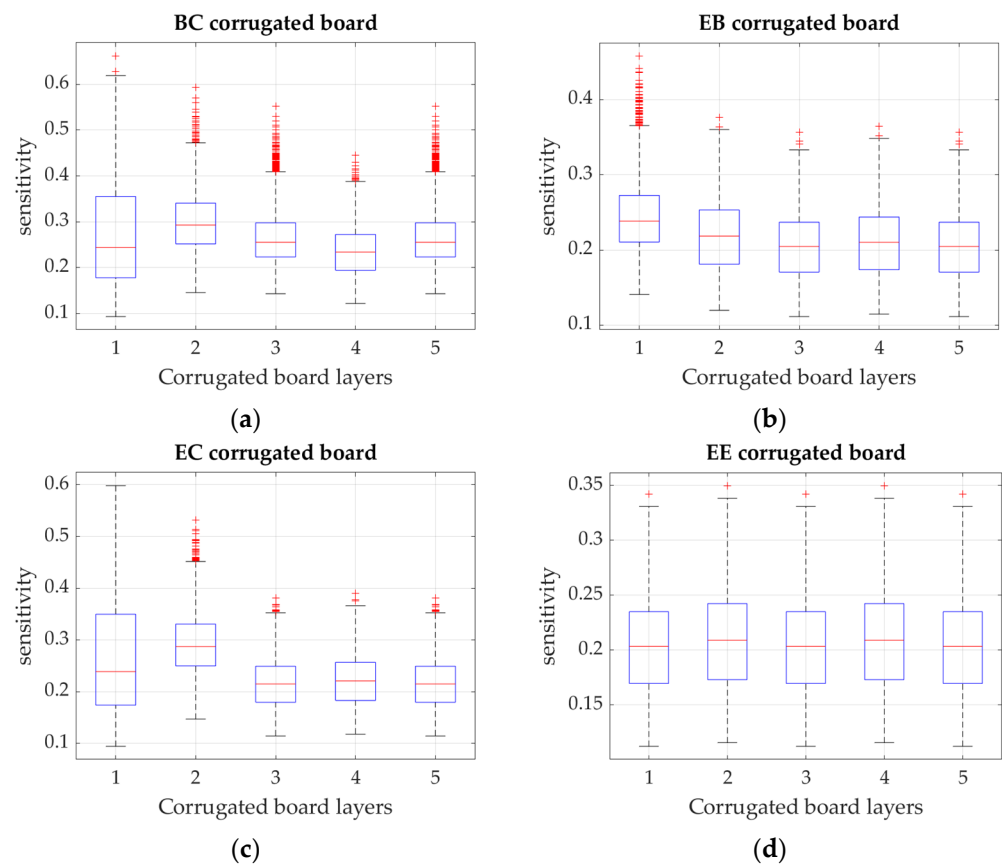


Figure 5. Sensitivity of ECT in relation to the layer grammage perturbation (1—bottom liner, 2—higher flute, 3—middle liner, 4—lower flute, 5—upper liner) for: (a) BC, (b) EB, (c) EC, and (d) EE corrugated cardboard.

Figures 6 and 7 show the sensitivities of ECT, P_{cr} , and BCT with respect to the grammage of the cardboard layers. The presented results are average values that were obtained from 120 boxes of various dimensions. The dimensions of the box base were from 100 × 100 mm to 500 × 300 mm, and the height of the box was in the range from 50 to 500 mm.

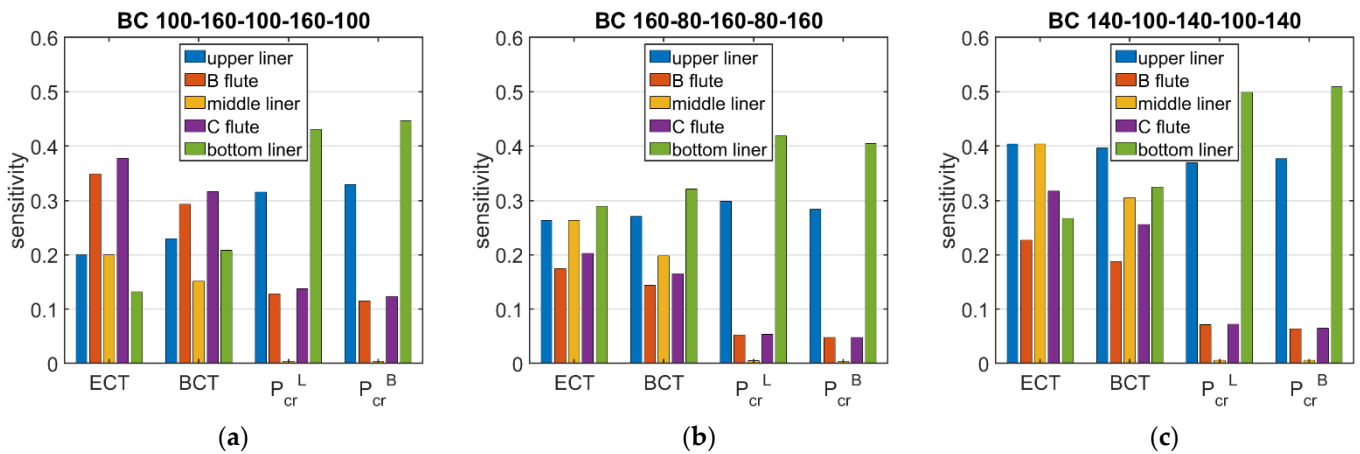


Figure 6. Average sensitivity of ECT, P_{cr} , and BCT of all boxes in relation to the layer grammage perturbation for BC cardboard of selected grades: (a) 100-160-100-160-100, (b) 160-80-160-80-160, and (c) 140-100-140-100-140.

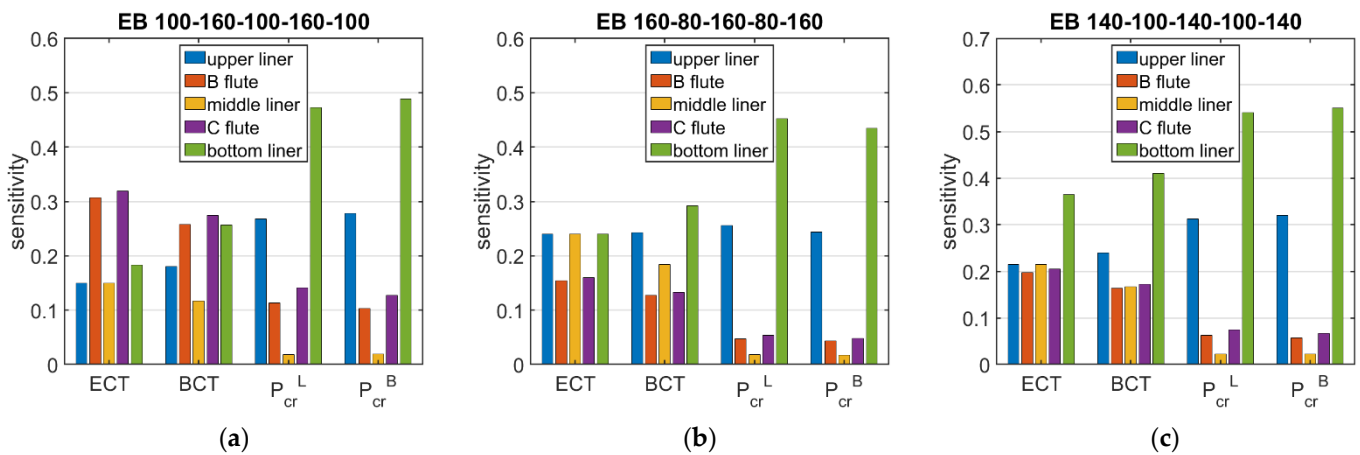


Figure 7. Average sensitivity of ECT, P_{cr} , and BCT of all boxes in relation to the layer grammage perturbation for EB cardboard of selected grades: (a) 100-160-100-160-100, (b) 160-80-160-80-160, and (c) 140-100-140-100-140.

The presented sensitivities are limited to three indices of corrugated cardboard—double-walled with a liner grammage of 100 g/m^2 and a fluting grammage of 160 g/m^2 —marked as 100-160-100-160-100, 160-80-160-80-160, and 140-100-140-100-140. The results are presented for the BC cardboard (see Figure 6) and the EB cardboard (see Figure 7).

Tables 3 and 4 show the sensitivity of BCT and P_{cr} depending on the bending stiffnesses for the BC and EB corrugated cardboards, respectively. The values in columns 3–5 are the average sensitivities computed for 36 boxes lower than 150 mm. The sensitivities in columns 6–8 are the average values obtained for nine packages higher than 400 mm, with a base dimension lower than 200 mm.

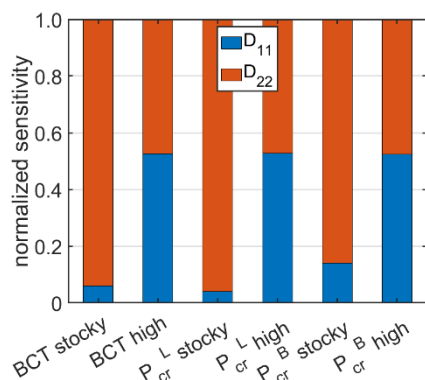
Figure 8 presents the participation of the bending stiffnesses D_{11} and D_{22} in the sensitivity of BCT and P_{cr} . The results are shown for the BC corrugated cardboard with a grade of 100-160-100-160-100. The proportions for the remaining cases are similar; therefore, the results are shown only for cardboard of one grade.

Table 3. Sensitivity of BCT and P_{cr} regarding the D_{11} and D_{22} perturbation of a BC corrugated cardboard.

Grade	Perturbed Parameter	Stocky Boxes			High Boxes		
		BCT	P_{cr}^L	P_{cr}^B	BCT	P_{cr}^L	P_{cr}^B
100-160-100-160-100	D_{11}	0.012	0.032	0.093	0.067	0.267	0.264
	D_{22}	0.183	0.775	0.571	0.060	0.239	0.240
160-80-160-80-160	D_{11}	0.015	0.041	0.116	0.062	0.248	0.245
	D_{22}	0.177	0.754	0.539	0.068	0.270	0.271
140-100-140-100-140	D_{11}	0.014	0.039	0.111	0.059	0.237	0.234
	D_{22}	0.178	0.759	0.547	0.070	0.278	0.280

Table 4. Sensitivity of BCT and P_{cr} regarding the D_{11} and D_{22} perturbation of an EB corrugated cardboard.

Grade	Perturbed Parameter	Stocky Boxes			High Boxes		
		BCT	P_{cr}^L	P_{cr}^B	BCT	P_{cr}^L	P_{cr}^B
100-160-100-160-100	D_{11}	0.012	0.034	0.098	0.069	0.277	0.274
	D_{22}	0.181	0.770	0.563	0.058	0.231	0.232
160-80-160-80-160	D_{11}	0.015	0.042	0.119	0.064	0.254	0.251
	D_{22}	0.176	0.752	0.535	0.066	0.265	0.266
140-100-140-100-140	D_{11}	0.014	0.040	0.114	0.061	0.244	0.241
	D_{22}	0.177	0.756	0.542	0.068	0.272	0.274

**Figure 8.** Normalized sensitivity of BCT and P_{cr} regarding the D_{11} and D_{22} perturbation of the BC corrugated cardboard with a grade of 100-160-100-160-100.

The above-presented results summarize the sensitivities calculated according to the scheme presented in Figure 4. Most analyses were based on simplified analytical formulas; only the part regarding the numerical homogenization used the basics of the finite element method. The homogenization method has already been extensively described in [45,49,50,61].

4. Discussion

This study is a continuation of the work recently presented by Mrówczyński et al. [2]. What distinguishes this work from the previous one is the attention to the effects related to imperfections in the asymmetrical cross section of a five-layer corrugated cardboard. Taking into account these effects and the other specificities of a five-layer corrugated cardboard allows for drawing slightly different, but still very important, conclusions. To the best of the authors' knowledge, there are no other scientific papers in the literature that describe in this way the influence of the composition of a corrugated board on all mechanical parameters of the structure of paper-based packaging. Therefore, the following discussion is limited to a summary of the observations of the results of this work.

The performed analyses allowed determining the sensitivity of ECT, P_{cr} , and BCT to small perturbations of the layer grammage and bending stiffnesses D_{11} and D_{22} . In Figure 5, the results of the ECT sensitivity for the four analyzed corrugated cardboards (BC, EB, EC, and EE) are presented. For asymmetrical cardboards, the grammage liner with a higher wave had a more important effect than the grammage of other liners (for BC cardboard, the sensitivity was similar). All cardboards with two different waves (flutes), were more sensitive to small changes in the grammage of the higher wave than to changes in the grammage of the lower wave. For the symmetrical EE cardboard, the sensitivity of liners and flutes was similar.

Figures 6 and 7 show the average sensitivities regarding the layer grammage perturbation for BC and EB cardboards, respectively. Based on of the presented results, it can be concluded that the sensitivities of the critical load of the longer and shorter walls of the box were very similar. The maximum difference between the average sensitivities was about 13%. It can be clearly seen that the value of the critical load was mostly influenced by the grammage of the external liners (from 2.44% to 5.51% when the liner grammage was changed by 10%), the fluting grammage had little influence (from 0.43% to 1.41% when changing the fluting grammage by 10%), and the influence of the middle liner grammage was negligible (from 0.04% to 0.22%).

Despite the low impact of the middle liner and fluting on the critical load of the walls, they contribute to the packaging load capacity through the ECT value, which is also a main component of the box strength (BCT). For corrugated cardboard with thick fluting (grade 100-160-100-160-100), both ECT and BCT were more sensitive to fluting perturbation than to liner perturbation. In the remaining cases (grades 160-80-160-80-160 and 140-100-140-100-140), the liners had a greater influence on the ECT and BCT values. In all cases, the external liners had a much greater impact on the load capacity than the middle liner (7% to 146%).

Tables 3 and 4 show the sensitivity of critical load and BCT to changes in the bending stiffness. It is easy to notice that the stiffness D_{11} is less important for stocky boxes than for slender ones. The change in BCT resulted from a change of D_{11} by 10% was about 0.14% for stocky boxes and about 0.64% for tall boxes. The opposite trend was observed for the stiffness D_{22} ; in fact, the change in BCT caused by a 10% change of D_{22} for low boxes was about 1.79%, while that for high boxes was about 0.65%. The same relationship was seen when analyzing the sensitivity of the critical load. Comparing the sensitivities to perturbations of both stiffnesses, it can be seen that for low boxes, the bending stiffness D_{22} is much more important than D_{11} , whereas for high boxes, both stiffnesses have a similar effect on the value of the load capacity and critical loads (see Figure 8).

5. Conclusions

Nowadays it is extremely important that materials are used in the best possible way in the production of various structures, including corrugated cardboard. Understanding and analyzing the impact of various factors on the load capacity of packaging is of key importance in the optimization process of both material consumption and selection of cardboard quality for a specific packaging structure. This paper presented the results obtained from numerical analyses of five-layer cardboard aimed at determining the sensitivity of certain values (indexes used to determine strength), such as edge crush resistance (ECT), critical load of the packaging walls (P_{cr}), and packaging load capacity (BCT), to changes in the grammage of the corrugated cardboard layers and bending stiffness D_{11} and D_{22} . Based on the performed numerical analyses and the presented calculation results, several conclusions were formulated, that will contribute to a more optimal design of double-walled corrugated cardboard packaging and thus improve the sustainable management of natural resources.

Author Contributions: Conceptualization, D.M. and T.G.; methodology, D.M. and T.G.; software, T.G. and D.M.; validation, D.M., A.K.-P. and T.G.; formal analysis, D.M.; investigation, D.M. and A.K.-P.; resources, D.M.; data curation, D.M.; writing—original draft preparation, A.K.-P., D.M. and T.G.; writing—review and editing, A.K.-P. and T.G.; visualization, D.M.; supervision, T.G.; project administration, T.G.; funding acquisition, A.K.-P. and T.G. All authors have read and agreed to the published version of the manuscript.

Funding: The APC was funded by the Ministry of Education and Science, Poland; the statutory funding at Poznan University of Life Sciences, grant number 506.569.05.00; and the statutory funding at Poznan University of Technology, grant number 0411/SBAD/0004.

Institutional Review Board Statement: Not applicable.

Informed Consent Statement: Not applicable.

Data Availability Statement: The data presented in this study are available on request from the corresponding author.

Acknowledgments: This article was created as a result of a cooperation, involving the internship of one of the co-authors, at the Department of Biosystem Engineering at the Poznan University of Life Sciences. The authors would like to thank the management of the Department of Biosystem Engineering and the Institute of Structural Analysis for making this cooperation possible and for partially co-financing this research.

Conflicts of Interest: The authors declare no conflict of interest.

References

1. Research Report: Paper & Paperboard Packaging Market, Report Code: PK 3496. Available online: <https://www.marketsandmarkets.com/Market-Reports/paper-paperboard-packaging-market-23392290.html> (accessed on 13 March 2022).
2. Mrówczyński, D.; Knitter-Piątkowska, A.; Garbowski, T. Non-Local Sensitivity Analysis and Numerical Homogenization in Optimal Design of Single-Wall Corrugated Board Packaging. *Materials* **2022**, *15*, 720. [CrossRef]
3. Kellicutt, K.; Landt, E. Development of design data for corrugated fibreboard shipping containers. *Tappi* **1952**, *35*, 398–402.
4. Maltenfort, G. Compression strength of corrugated containers. *Fibre Contain* **1956**, *41*, 106–121.
5. McKee, R.C.; Gander, J.W.; Wachuta, J.R. Compression strength formula for corrugated boxes. *Paperboard Packag.* **1963**, *48*, 149–159.
6. Sohrabpour, V.; Hellström, D. Models and software for corrugated board and box design. In Proceedings of the 18th International Conference on Engineering Design (ICED 11), Copenhagen, Denmark, 15–18 October 2011.
7. Schramper, K.E.; Whitsitt, W.J.; Baum, G.A. *Combined Board Edge Crush (ECT) Technology*; Institute of Paper Chemistry: Appleton, WI, USA, 1987.
8. Batelka, J.J.; Smith, C.N. *Package Compression Model*; Institute of Paper Science and Technology, Georgia Institute of Technology: Atlanta, GA, USA, 1993.
9. Urbanik, T.J.; Frank, B. Box compression analysis of world-wide data spanning 46 years. *Wood Fiber Sci.* **2006**, *38*, 399–416.
10. Avilés, F.; Carlsson, L.A.; May-Pat, A. A shear-corrected formulation of the sandwich twist specimen. *Exp. Mech.* **2012**, *52*, 17–23. [CrossRef]
11. Garbowski, T.; Gajewski, T.; Grabski, J.K. The role of buckling in the estimation of compressive strength of corrugated cardboard boxes. *Materials* **2020**, *13*, 4578. [CrossRef] [PubMed]
12. Garbowski, T.; Knitter-Piątkowska, A. Analytical Determination of the Bending Stiffness of a Five-Layer Corrugated Cardboard with Imperfections. *Materials* **2022**, *15*, 663. [CrossRef]
13. Domaneschi, M.; Perego, U.; Borgqvist, E.; Borsari, R. An industry-oriented strategy for the finite element simulation of paperboard creasing and folding. *Packag. Technol. Sci.* **2017**, *30*, 269–294. [CrossRef]
14. Awais, M.; Tanninen, P.; Leppänen, T.; Matthews, S.; Sorvari, J.; Varis, J.; Backfol, K. A computational and experimental analysis of crease behavior in press forming process. *Procedia Manuf.* **2018**, *17*, 835–842. [CrossRef]
15. Thakkar, B.K.; Gooren, L.G.J.; Peerlings, R.H.J.; Geers, M.G.D. Experimental and numerical investigation of creasing in corrugated paperboard. *Philos. Mag.* **2008**, *88*, 3299–3310. [CrossRef]
16. Beex, L.A.A.; Peerlings, R.H.J. An experimental and computational study of laminated paperboard creasing and folding. *Int. J. Solids Struct.* **2009**, *46*, 4192–4207. [CrossRef]
17. Giampieri, A.; Perego, U.; Borsari, R. A constitutive model for the mechanical response of the folding of creased paperboard. *Int. J. Solids Struct.* **2011**, *48*, 2275–2287. [CrossRef]
18. Leminen, V.; Tanninen, P.; Pesonen, A.; Varis, J. Effect of mechanical perforation on the press-forming process of paperboard. *Procedia Manuf.* **2019**, *38*, 1402–1408. [CrossRef]
19. Garbowski, T.; Jarmuszcak, M. Numerical strength estimate of corrugated board packages. Part 1. Theoretical assumptions in numerical modeling of paperboard packages. *Pol. Pap. Rev.* **2014**, *70*, 219–222. (In Polish)

20. Garbowski, T.; Jarmuszczyk, M. Numerical strength estimate of corrugated board packages. Part 2. Experimental tests and numerical analysis of paperboard packages. *Pol. Pap. Rev.* **2014**, *70*, 277–281. (In Polish)
21. Park, J.; Chang, S.; Jung, H.M. Numerical prediction of equivalent mechanical properties of corrugated paperboard by 3D finite element analysis. *Appl. Sci.* **2020**, *10*, 7973. [[CrossRef](#)]
22. Park, J.; Park, M.; Choi, D.S.; Jung, H.M.; Hwang, S.W. Finite element-based simulation for edgewise compression behavior of corrugated paperboard for packing of agricultural products. *Appl. Sci.* **2020**, *10*, 6716. [[CrossRef](#)]
23. Ganiy, A.; Ye, Y.; Ping, H.; Wen-bin, H.; Xiao, H. Analysis of the performance of adhesively bonded corrugated core sandwich structures using cohesive zone method. *J. Sandw. Struct. Mater.* **2020**, *22*, 104–124. [[CrossRef](#)]
24. Xiao, H.; Ganiy, A.; Ping, H.; Wen-bin, H.; Yermek, B.; Mazhit, A. Numerical prediction on the mechanical degradation of adhesively bonded corrugated sandwich beam after hygrothermal ageing. *Comp. Struct.* **2020**, *241*, 112131. [[CrossRef](#)]
25. Nordstrand, T. Basic Testing and Strength Design of Corrugated Board and Containers. Ph.D. Thesis, Lund University, Lund, Sweden, 2003.
26. Nordstrand, T.; Carlsson, L. Evaluation of transverse shear stiffness of structural core sandwich plates. *Comp. Struct.* **1997**, *37*, 145–153. [[CrossRef](#)]
27. Słonina, M.; Dziurka, D.; Smardzewski, J. Experimental research and numerical analysis of the elastic properties of paper cell cores before and after impregnation. *Materials* **2020**, *13*, 2058. [[CrossRef](#)] [[PubMed](#)]
28. Czechowski, L.; Kmita-Fudalej, G.; Szewczyk, W.; Galewski, J.; Bienkowska, M. Numerical and experimental study of five-layer non-symmetrical paperboard panel stiffness. *Materials* **2021**, *14*, 7453. [[CrossRef](#)] [[PubMed](#)]
29. Jamsari, M.A.; Kueh, C.; Gray-Stuart, E.M.; Dahm, K.; Bronlund, J.E. Experimental and numerical performance of corrugated fibreboard at different orientations under four-point bending test. *Packag. Technol. Sci.* **2019**, *32*, 555–565. [[CrossRef](#)]
30. Urbanik, T.J.; Saliklis, E.P. Finite element corroboration of buckling phenomena observed in corrugated boxes. *Wood Fiber Sci.* **2003**, *35*, 322–333.
31. Hallbäck, N.; Korin, C.; Barbier, C.; Nygård, M. Finite element analysis of hot melt adhesive joints in carton board. *Packag. Technol. Sci.* **2014**, *21*, 701–712. [[CrossRef](#)]
32. Allaoui, S.; Benzeggagh, M.L.; Aboura, Z.; Talbi, N. Elastic behaviour of corrugated cardboard: Experiments and modeling. *Comp. Struct.* **2004**, *63*, 53–62.
33. Biancolini, M.E. Evaluation of equivalent stiffness properties of corrugated board. *Comp. Struct.* **2005**, *69*, 322–328. [[CrossRef](#)]
34. Ramírez-Torres, A.; Penta, R.; Rodríguez-Ramos, R.; Merodio, J.; Sabina, F.J.; Bravo-Castillero, J.; Guinovart-Díaz, R.; Preziosi, L.; Grillo, A. Three scales asymptotic homogenization and its application to layered hierarchical hard tissues. *Int. J. Solids Struct.* **2018**, *130–131*, 190–198. [[CrossRef](#)]
35. Ramírez-Torres, A.; Di Stefano, S.; Grillo, A.; Rodríguez-Ramos, R.; Merodio, J.; Penta, R. An asymptotic homogenization approach to the microstructural evolution of heterogeneous media. *Int. J. Non Linear Mech.* **2018**, *106*, 245–257. [[CrossRef](#)]
36. Garbowski, T.; Jarmuszczyk, M. Homogenization of corrugated paperboard. Part 1. Analytical homogenization. *Pol. Pap. Rev.* **2014**, *70*, 345–349. (In Polish)
37. Garbowski, T.; Jarmuszczyk, M. Homogenization of corrugated paperboard. Part 2. Numerical homogenization. *Pol. Pap. Rev.* **2014**, *70*, 390–394. (In Polish)
38. Garbowski, T.; Marek, A. Homogenization of corrugated boards through inverse analysis. In Proceedings of the 1st International Conference on Engineering and Applied Sciences Optimization, Kos Island, Greece, 4–6 June 2014; pp. 1751–1766.
39. Hohe, J. A direct homogenization approach for determination of the stiffness matrix for microheterogeneous plates with application to sandwich panels. *Compos. Part B* **2003**, *34*, 615–626. [[CrossRef](#)]
40. Buannic, N.; Cartraud, P.; Quesnel, T. Homogenization of corrugated core sandwich panels. *Comp. Struct.* **2003**, *59*, 299–312. [[CrossRef](#)]
41. Abbès, B.; Guo, Y.Q. Analytic homogenization for torsion of orthotropic sandwich plates. *Appl. Comp. Struct.* **2010**, *92*, 699–706. [[CrossRef](#)]
42. Gallo, J.; Cortés, F.; Alberdi, E.; Goti, A. Mechanical behavior modeling of containers and octabins made of corrugated cardboard subjected to vertical stacking loads. *Materials* **2021**, *14*, 2392. [[CrossRef](#)] [[PubMed](#)]
43. Suarez, B.; Muneta, M.L.M.; Sanz-Bobi, J.D.; Romero, G. Application of homogenization approaches to the numerical analysis of seating made of multi-wall corrugated cardboard. *Compos. Struct.* **2021**, *262*, 113642. [[CrossRef](#)]
44. Nguyen-Minh, N.; Tran-Van, N.; Bui-Xuan, T.; Nguyen-Thoi, T. Static analysis of corrugated panels using homogenization models and a cell-based smoothed mindlin plate element (CS-MIN3). *Front. Struct. Civ. Eng.* **2019**, *13*, 251–272. [[CrossRef](#)]
45. Garbowski, T.; Gajewski, T. Determination of transverse shear stiffness of sandwich panels with a corrugated core by numerical homogenization. *Materials* **2021**, *14*, 1976. [[CrossRef](#)] [[PubMed](#)]
46. Archaviboonyobul, T.; Chaveesuk, R.; Singh, J.; Jinkarn, T. An analysis of the influence of hand hole and ventilation hole design on compressive strength of corrugated fiberboard boxes by an artificial neural network model. *Packag. Technol. Sci.* **2020**, *33*, 171–181. [[CrossRef](#)]
47. Jamsari, M.A.; Kueh, C.; Gray-Stuart, E.M.; Dahm, K.; Bronlund, J.E. Modelling the impact of crushing on the strength performance of corrugated fibreboard. *Packag. Technol. Sci.* **2020**, *33*, 159–170. [[CrossRef](#)]
48. Bai, J.; Wang, J.; Pan, L.; Lu, L.; Lu, G. Quasi-static axial crushing of single wall corrugated paperboard. *Compos. Struct.* **2019**, *226*, 111237. [[CrossRef](#)]

49. Gajewski, T.; Garbowski, T.; Staszak, N.; Kuca, M. Crushing of Double-Walled Corrugated Board and Its Influence on the Load Capacity of Various Boxes. *Energies* **2021**, *14*, 4321. [[CrossRef](#)]
50. Garbowski, T.; Gajewski, T.; Mrówczyński, D.; Jędrzejczak, R. Crushing of Single-Walled Corrugated Board during Converting: Experimental and Numerical Study. *Energies* **2021**, *14*, 3203. [[CrossRef](#)]
51. Garbowski, T.; Grabski, J.K.; Marek, A. Full-field measurements in the edge crush test of a corrugated board—Analytical and numerical predictive models. *Materials* **2021**, *14*, 2840. [[CrossRef](#)] [[PubMed](#)]
52. Garbowski, T.; Knitter-Piątkowska, A.; Marek, A. New edge crush test configuration enhanced with full-field strain measurements. *Materials* **2021**, *14*, 5768. [[CrossRef](#)]
53. Hägglund, R.; Åslund, P.E.; Carlsson, L.A.; Isaksson, P. Measuring thickness changes of edgewise compression loaded corrugated board panels using digital image correlation. *J. Sandw. Struct. Mater.* **2010**, *14*, 75–94. [[CrossRef](#)]
54. Viguié, J.; Dumont, P.J.J.; Vacher, P.; Orgéas, L.; Desloges, I.; Mauret, E. Analysis of the strain and stress field of cardboard box during compression by 3D Digital Image Correlation. *Appl. Mech. Mater.* **2010**, *24–25*, 103–108. [[CrossRef](#)]
55. Viguié, J.; Dumont, P.J.J.; Orgéas, L.; Vacher, P.; Desloges, I.; Mauret, E. Surface stress and strain fields on compressed panels of corrugated board boxes. An experimental analysis by using Digital Image Stereocorrelation. *Comp. Struct.* **2011**, *93*, 2861–2873. [[CrossRef](#)]
56. Viguié, J.; Dumont, P.J.J. Analytical post-buckling model of corrugated board panels using digital image correlation measurements. *Comp. Struct.* **2013**, *101*, 243–254. [[CrossRef](#)]
57. Fadji, T.; Coetzee, C.J.; Opara, U.L. Evaluating the displacement field of paperboard packages subjected to compression loading using digital image correlation (DIC). *Food Bioprod. Process.* **2020**, *123*, 60–71. [[CrossRef](#)]
58. Maier, G.; Bolzon, G.; Buljak, V.; Garbowski, T.; Miller, B. Synergic combinations of computational methods and experiments for structural diagnoses. In *Computer Methods in Mechanics*; Kuczma, M., Wilmanski, K., Eds.; Advanced Structured Materials; Springer: Berlin/Heidelberg, Germany, 2010; Volume 1, pp. 453–476.
59. Frank, B. Corrugated box compression—A literature survey. *Packag. Technol. Sci.* **2014**, *27*, 105–128. [[CrossRef](#)]
60. Garbowski, T.; Gajewski, T.; Grabski, J.K. Estimation of the compressive strength of corrugated cardboard boxes with various perforations. *Energies* **2021**, *14*, 1095. [[CrossRef](#)]
61. Garbowski, T.; Knitter-Piątkowska, A.; Mrówczyński, D. Numerical homogenization of multi-layered corrugated cardboard with creasing or perforation. *Materials* **2021**, *14*, 3786. [[CrossRef](#)] [[PubMed](#)]
62. Gong, G.; Liu, Y.; Fan, B.; Sun, D. Deformation and compressive strength of corrugated cartons under different indentation shapes: Experimental and simulation study. *Packag. Technol. Sci.* **2020**, *33*, 215–226. [[CrossRef](#)]
63. Fadji, T.; Coetzee, C.J.; Opara, U.L. Compression strength of ventilated corrugated paperboard packages: Numerical modelling, experimental validation and effects of vent geometric design. *Biosyst. Eng.* **2016**, *151*, 231–247. [[CrossRef](#)]
64. Fadji, T.; Ambaw, A.; Coetzee, C.J.; Berry, T.M.; Opara, U.L. Application of finite element analysis to predict the mechanical strength of ventilated corrugated paperboard packaging for handling fresh produce. *Biosyst. Eng.* **2018**, *174*, 260–281. [[CrossRef](#)]
65. Mrówczyński, D.; Garbowski, T.; Knitter-Piątkowska, A. Estimation of the compressive strength of corrugated board boxes with shifted creases on the flaps. *Materials* **2021**, *14*, 5181. [[CrossRef](#)] [[PubMed](#)]
66. Zhang, Y.-L.; Chen, J.; Wu, Y.; Sun, J. Analysis of hazard factors of the use of corrugated carton in packaging low-temperature yogurt during logistics. *Procedia Environ. Sci.* **2011**, *10*, 968–973. [[CrossRef](#)]
67. Hung, D.; Nakano, Y.; Tanaka, F.; Hamanaka, D.; Uchino, T. Preserving the strength of corrugated cardboard under high humidity condition using nano-sized mists. *Compos. Sci. Technol.* **2010**, *70*, 2123–2127. [[CrossRef](#)]
68. Böröcz, P.; Molnár, B. Measurement and analysis of vibration levels in stacked small package shipments in delivery vans as a function of free movement space. *Appl. Sci.* **2020**, *10*, 7821. [[CrossRef](#)]
69. Quesenberry, C.; Horvath, L.; Bouldin, J.; White, M.S. The Effect of pallet top deck stiffness on the compression strength of asymmetrically supported corrugated boxes. *Packag. Technol. Sci.* **2020**, *33*, 547–558. [[CrossRef](#)]
70. Mondi Technical Data. Available online: <https://www.mondigroup.com/en/products-and-solutions/containerboard/containerboard-products/> (accessed on 13 March 2022).
71. Baum, G.A.; Brennan, D.C.; Habeger, C.C. Orthotropic elastic constants of paper. *Tappi* **1981**, *64*, 97–101.
72. Mann, R.W.; Baum, G.A.; Habeger, C.C. Determination of all nine orthotropic elastic constants for machine-made paper. *Tappi* **1980**, *63*, 163–166.